

High Q^2 -Anomaly at HERA and Supersymmetry

H. Dreiner¹ and P. Morawitz²

¹ Rutherford Lab., Chilton, Didcot, OX11 0QX, UK

² Imperial College, HEP Group, London SW7 2BZ, UK

Abstract

We discuss the recently observed excess of high lepton momentum transfer, Q^2 , neutral current deep inelastic scattering events at HERA in the light of supersymmetry with broken R-parity. We find more than one possible solution. We consider the possibilities for testing these hypotheses at HERA, the Tevatron and at LEP. One lepton-number violating operator can account for both the HERA data and the four-jet anomaly seen by ALEPH at LEP.

1 Introduction

Recently both experiments at HERA have quoted an excess at high lepton momentum transfer, Q^2 , in their neutral current deep inelastic scattering (NC DIS) data [1, 2]. For $Q^2 > 15,000 \text{ GeV}^2$, *H1* have found 12 events where they expect ≈ 5 from the Standard Model (SM) [1]. For $Q^2 > 20,000 \text{ GeV}^2$ *ZEUS* observe 5 events where they expect ≈ 2 from the SM [2]. In addition, *H1* have seen a slight excess in their charged current deep inelastic scattering (CC DIS) [1]. Due to the low rate, we find it is still too early to comment on this. The NC DIS discrepancies could be the first hint of physics beyond the SM [3]. There have been three main suggestions predicting an excess of events at high Q^2 at HERA: contact interactions [4, 5, 6], leptoquarks [7, 8], and supersymmetry with broken R-parity [9, 10, 11, 12].

If quarks (or leptons) have a substructure this could lead to an excess of events at high values of Q^2 at colliders. A four-fermion operator based analysis for testing effective theories at e^+e^- -colliders was first proposed in Ref.[4]. This analysis of contact interactions was generalised to eP deep inelastic scattering in [5] where the operators are of the form $eeqq$. Contact interactions are a parametrisation of unknown physics at a higher energy scale ($\Lambda \gg \sqrt{s}$) via gauge-invariant but non-renormalisable operators. At HERA, they can lead to an increase or a depletion of high Q^2 events, depending on the sign of the interference with the SM-interaction, which is a free parameter. These events should not show any peak-like structure, since the HERA energy is well below any supposed resonances. At HERA, one can attempt to extract the unknown scale of the new physics. This analysis is typically performed one-operator at a time. But it is also possible to consider combined effects [6]. This should be done with the present HERA data, but we do not further consider this possibility here.

Both leptoquarks and supersymmetry with broken R-parity predict s-channel resonances in positron-proton scattering. In Grand Unified Models, the leptoquarks are typically heavy and well beyond the reach of colliders [13]. However, there is a set of models which predict low-energy leptoquarks [14]. A systematic search for such leptoquarks was first proposed in Ref.[7] and subsequently much effort has been dedicated at HERA to this search [8]. Within supersymmetry, we naturally expect all new states to have masses between 100 GeV and 1 TeV in order to maintain the solution to the gauge hierarchy problem [15]. Depending on the magnitude of the Yukawa coupling and the remaining supersymmetry spectrum, squarks can behave just like leptoquarks at HERA. But squarks can naturally have further decay modes and their discussion is thus more general. In the following, we focus on the implications of the recent HERA data for supersymmetry with broken R-parity. When relevant we shall emphasise below where the leptoquark description is distinct.

In Section 2 we briefly review supersymmetry with broken R-parity and focus on the relevant terms for HERA. In Section 3 we review the indirect bounds on these operators.

In Section 4 we determine which R-parity violating operators could possibly lead to the observed excess at HERA while still being consistent with the existing indirect bounds. In Sections 5 through 7 we discuss how these operators could be tested in future runs at HERA, as well as with present and upcoming data at LEP and at the Tevatron. In Section 8 we present our conclusions. In the Appendix we have collected some of the relevant formula for completeness.

2 Supersymmetry with Broken R-Parity at HERA

When minimally extending the particle content of the SM to incorporate supersymmetry one must add an extra Higgs $SU(2)_L$ doublet and then double the particle content. The most general interactions of these particles consistent with supersymmetry and $SU(3)_c \times SU(2)_L \times U(1)_Y$ gauge symmetry are those of the minimal supersymmetric standard model (MSSM) [16] as well as the superpotential terms¹[18]

$$\lambda_{ijk} L_i L_j \bar{E}_k + \lambda'_{ijk} L_i Q_j \bar{D}_k + \lambda''_{ijk} \bar{U}_i \bar{D}_j \bar{D}_k. \quad (1)$$

Here L (Q) is the lepton (quark) doublet superfield, and \bar{D}, \bar{U} (\bar{E}) are the down-like and up-like quark (lepton) singlet superfields, respectively. $i, j, k = 1, 2, 3$ are generation indices. The last two sets of terms in (1) lead to rapid proton decay [19]. The solution of this problem in the MSSM is to impose R-parity,

$$R_p = (-1)^{3B+L+2S}, \quad (2)$$

a multiplicative discrete symmetry. Here B denotes baryon number, L lepton number² and S the spin of a field. All SM fields have $R_p = +1$; their supersymmetric partners have $R_p = -1$. This solution is not unique. There are many models which protect the proton but allow a subset of the terms in (1) [17, 20, 21]. This subset can be as small as two operators even for a gauge symmetry [20]. All these alternative solutions are denoted ‘‘R-parity violation’’. In the following, we shall focus on the subset of the operators (1)

$$\lambda'_{1jk} L_1 Q_j \bar{D}_k. \quad (3)$$

At HERA these operators can lead to resonant squark production

$$e^+ + \bar{u}_j \rightarrow \tilde{d}_k, \quad (4)$$

$$e^+ + d_k \rightarrow \tilde{u}_j. \quad (5)$$

This was first proposed by J. Hewett in Ref.[9] where she considered the direct R-parity violating decay of the squark to the initial state. The processes (4,5) were discussed in more

¹There is the further term $\kappa_i L_i H_u$ which violates lepton number. If the soft-breaking terms are universal it can be rotated away [17].

²This should not lead to any confusion with the lepton doublet superfield, L , of Eq.(1).

λ'_{111}	λ'_{112}	λ'_{113}	λ'_{121}	λ'_{122}	λ'_{123}	λ'_{131}	λ'_{132}	λ'_{133}
0.001 ^(a)	0.03 ^(b)	0.03 ^(b)	0.06 ^(c)	0.06 ^(d)	0.26 ^(e)	0.06 ^(c)	0.63 ^(f)	0.002 ^(d)
0.004	0.06	0.06	0.13	0.087	0.55	0.13	1.3	0.003

Table 1: Indirect bounds on first lepton generation operators $LQ\bar{D}$. The first line is the bound for a scalar fermion mass of 100 GeV the second line for 210 GeV . The bounds derive from the following physical processes: ^(a) neutrinoless double beta decay [26], ^(b) charged current universality [27, 28, 29], ^(c) atomic parity violation [28, 30, 29], ^(d) ν_e mass [31], ^(e) forward backward asymmetry [27], and ^(f) D-decays [32]. The bounds from ^(b), ^(c), ^(e), and ^(f) scale linearly with the squark mass $(\tilde{M}_{\tilde{q}}/100)\text{ GeV}$. The bound from ^(d) scales with the square root $\sqrt{\tilde{M}_{\tilde{q}}/100\text{ GeV}}$. The bound ^(a) scales as $(\tilde{M}_{\tilde{q}}/100\text{ GeV})^2\sqrt{\tilde{M}_{\tilde{g}}/100\text{ GeV}}$. We have conservatively estimated the gluino mass at $\tilde{M}_{\tilde{g}} = 1\text{ TeV}$. We have given the 1 sigma bounds.

detail in [10, 11] where the squark cascade decays via a photino were included. This enables the distinction from a leptoquark, depending on the supersymmetric spectrum. The full mixing in the neutralino sector was first considered in [22] for R-parity violation at HERA. For a scalar top quark ($j = 3$), the decays via the neutralino are kinematically forbidden. This scenario was discussed in considerable detail by T. Kon *et al.* [12, 23]. The squark decays for the full gaugino mixing including the chargino were discussed by E. Perez [24] and in a shorter version in [25]. This enabled a full classification of the final state topologies at HERA.

Making use of all this work, we wish to determine the size and generation structure j, k of the coupling λ'_{1jk} of (3) which is preferred by the HERA data. We would also like to consider the best estimate for the squark mass. However, in order to do that we must first consider the indirect bounds on the couplings λ'_{1jk} .

3 Previous Indirect Bounds

The operators (3) can contribute to several processes with initial and final state SM particles via the exchange of virtual sleptons or squarks. Since to date all such processes have been observed in agreement with the SM, this leads to upper bounds on all the couplings which we summarise in Table 1. We give the bounds for a scalar fermion mass of 100 GeV , which is the standard, and 210 GeV , which is what we require below. These two bounds are related via scaling properties which are explicitly given in the table caption. We have updated some previous bounds using more recent data from the PDG [29]. The bound from atomic parity violation is obtained using the “weak charge”, Q_W , [29] and was not previously applied to R-parity violation [28]. All but two of the bounds are well below the electromagnetic coupling.

There is a further set of stringent bounds from the decay $K \rightarrow \pi\nu\nu$ [33].

$$\lambda'_{1jk} < 0.012, \quad j = 1, 2, \quad k = 1, 2, 3; \quad \tilde{M} = 100 \text{ GeV}, \quad (6)$$

$$\lambda'_{132} < 0.19, \quad \tilde{M} = 100 \text{ GeV}. \quad (7)$$

These limits scale linearly with the squark mass. However, these bounds are model dependent. If the absolute mixing of the quarks (not squarks) is purely in the down-quark sector then these bounds apply. If it is purely in the up-quark sector then these bounds revert to those of Table 1. In order to keep an open mind to all *possible* solutions we do not further consider these model dependent bounds.

If there is a charged, first or second generation doublet slepton ($\tilde{e}_L, \tilde{\mu}_L$) lighter than the top quark there is an additional bound from top quark decays [33]

$$\lambda'_{132} < 0.4, \quad M_{\tilde{\ell}} = 100 \text{ GeV}, \quad (8)$$

which is more strict than the one given in Table 1.

H1 have performed a direct search for supersymmetry with broken R-parity [34]. The bounds from this search depend on the neutralino mass. For a neutralino mass $M_{\tilde{\chi}_1^0} = 40 \text{ GeV} < M_{\tilde{q}}$ they obtain

$$\lambda'_{1j1} < 0.2, \quad M_{\tilde{q}} = 200 \text{ GeV}, \quad M_{\tilde{\chi}_1^0} = 40, \quad (9)$$

$$\lambda'_{132} < 0.22, \quad M_{\tilde{q}} = 150 \text{ GeV}, \quad M_{\tilde{\chi}_1^0} = 80. \quad (10)$$

In particular the last bound is significantly better than the indirect bound of Table 1, but is also model dependent.

4 HERA's high Q^2 excess interpreted as s-channel squark production

4.1 R-parity Violating Squark Decays

We would now like to interpret the observed excess at HERA in terms of supersymmetry with R-parity violation. For this, we combine the *H1* and *ZEUS* data in order to compare it more easily with different R-parity violating models. For $Q^2 > 20,000 \text{ GeV}^2$, *H1* and *ZEUS* see a total of 10 events [1, 2], where 4.08 ± 0.36 events are expected from SM contributions [35]. The total integrated luminosity of the two experiments is 34.3 pb^{-1} , which translates into an excess cross-section over the SM expectation of

$$\sigma_{ex}(Q^2 > 20,000 \text{ GeV}^2) = (0.17 \pm 0.07(\text{stat})) \text{ pb}. \quad (11)$$

In Figures 1 and 2 we show this combined excess cross section as a horizontal band.

The combined reconstructed values of the hypothetical squark mass $M_{\tilde{q}}$ (where $M_{\tilde{q}}$ is related to Bjorken-x by $M_{\tilde{q}}^2 = xs$ and s is the centre-of-mass energy squared) show some spread between the two experiments ($M_{\tilde{q}} = 200 \text{ GeV}$ for *H1*, $M_{\tilde{q}} = 220 \text{ GeV}$ for *ZEUS*). Combining the two experiments, we obtain³

$$M_{\tilde{q}} = (210 \pm 20) \text{ GeV}, \quad (12)$$

as our best estimate.

In order to determine the contribution from R-parity violation we consider one of the operators (3) at a time while assuming the others are negligible. For a given non-vanishing operator $\lambda'_{1jk} L_1 Q_j \bar{D}_k$, the produced \tilde{u}_j , or \tilde{d}_k squark can have many decay modes, depending on the mass spectrum of the supersymmetric particles [10, 11, 24, 25, 36]. For all SUSY spectra, the squark can decay via the operator itself resulting in the interactions

$$e^+ + \bar{u}_j \rightarrow \tilde{d}_k \rightarrow e^+ + \bar{u}_j, \quad (13)$$

$$e^+ + \bar{u}_j \rightarrow \tilde{d}_k \rightarrow \bar{\nu} + \bar{d}_j, \quad (14)$$

$$e^+ + d_k \rightarrow \tilde{u}_j \rightarrow e^+ + d_k, \quad (15)$$

at HERA. The first and third have equivalent initial and final states to NC DIS and can thus contribute to the observed excess. Analogously, the second can contribute to CC DIS. Let us for now assume these are the only decay modes of the produced \tilde{u}_j or \tilde{d}_k squark. We then compute the production cross section using [9, 11] and the *MRS*G structure functions [37]. For (13) and (14) we include the extra contribution to the width for the other decay mode. The correction to the narrow width approximation by using the full resonance width is $\lesssim 10\%$.

In Figure 1, we plot the production cross section $\sigma(e^+ + d_k \rightarrow \tilde{u}_j \rightarrow e^+ + d_k)$ for $Q^2 > 20,000 \text{ GeV}$ as a function of the R-parity violating couplings λ'_{1j1} , λ'_{1j2} , λ'_{1j3} . For each coupling, the three curves are for the squark masses $M_{\tilde{u}_j} = 200, 210, \text{ and } 220 \text{ GeV}$ from top to bottom, respectively. The cross section is largest for λ'_{1j1} due to the incoming valence quark. The other two cross sections are suppressed because of the significantly smaller strange and bottom sea-quark structure functions $s(x)$, $b(x)$.

In Figure 2, we analogously plot the cross sections $\sigma(e^+ + \bar{u}_j \rightarrow \tilde{d}_k \rightarrow e^+ + \bar{u}_j)$ as a function of the couplings λ'_{11k} and λ'_{12k} for the three squark mass values $M_{\tilde{d}_k} = 200, 210, \text{ and } 220 \text{ GeV}$. Here, we have included the full R-parity violating width from the two \tilde{d}_j decay modes. These cross sections are both suppressed because of the small up and charm sea-structure functions $\bar{u}(x)$ and $\bar{c}(x)$, respectively, as well as the increased width. There

³The errors quoted on the mass of the excess events (M_e) in Table 6 [1] is not the actual error on the reconstructed mass of any supposed resonance. This error is most likely larger as can be seen from the broad width of the distributions in Fig. 2b of Ref. [1]. Analogous, remarks apply to the ZEUS analysis [2]. We therefore feel justified in combining the data in this way.

is no contribution for λ'_{13k} because of the unknown and suppressed top-quark structure function, $\bar{t}(x)$.

We now compare the plotted cross sections with the hatched band of Eq.(11), and the bounds in the second row of Table 1. We obtain the following set of solutions where R-parity violation can explain the excess in the HERA data

$$\begin{aligned}
(1) \quad & \lambda'_{121} \approx 0.04, \quad \tilde{c}, \quad M_{\tilde{c}} = (210 \pm 20) \text{ GeV}, \\
(2) \quad & \lambda'_{123} \gtrsim 0.4, \quad \tilde{c}, \quad M_{\tilde{c}} < 210 \text{ GeV}, \\
(3) \quad & \lambda'_{123} \gtrsim 0.4, \quad \tilde{b}, \quad M_{\tilde{b}} < 210 \text{ GeV}, \\
(4) \quad & \lambda'_{131} \approx 0.04, \quad \tilde{t}, \quad M_{\tilde{t}} = (210 \pm 20) \text{ GeV}, \\
(5) \quad & \lambda'_{132} \gtrsim 0.3, \quad \tilde{t}, \quad M_{\tilde{t}} = (210 \pm 20) \text{ GeV}.
\end{aligned} \tag{16}$$

In each row we first present the approximate value of the required Yukawa coupling, then denote the produced squark and the mass range of the squark which is viable. Thus we obtain many solutions; however, the preferred solutions which are well within the constraints are (16.1), (16.4) and (16.5) with a produced scalar charm quark and a scalar top quark (“stop”), respectively. Before discussing the other squark decay modes, we note that within supersymmetric unification scenarios there is a possibility for a very light stop, possibly even the LSP [38]. For a stop-LSP, the process (15) would be the only decay.

There is one possible further solution, which is intriguing. Combining the solutions (16.2) and (16.3), it is possible that HERA has produced two different squarks: a scalar charm *and* a scalar bottom. The required coupling is then reduced by a factor $\sqrt{2}$ to $\lambda'_{123} \approx 0.28$, which is well away from the indirect bound.

$$(7) \quad \lambda'_{123} = 0.28, \quad \tilde{c} \ \& \ \tilde{b}, \quad M_{\tilde{q}} \approx 210 \text{ GeV}. \tag{17}$$

We make one further point [39]. The leading order QCD correction to the resonant squark production is presently not known. On-shell squark production is effectively a $2 \rightarrow 1$ process for which the QCD corrections are typically positive and large [40]. If this is indeed the case for resonant squark production at HERA this would give additional leeway in the Yukawa-coupling for the more marginal solutions. The required coupling would be reduced to λ'/\sqrt{K} , where K is the QCD K -factor.

4.2 Gaugino Decays of the Squark

In this Subsection we wish to discuss the case where the produced squark is not the LSP and can thus have further supersymmetric decay modes. (This section has no analogy for leptoquarks.) As noted above, supersymmetry dramatically extends the spectrum of the SM. It is way beyond the scope of this paper to perform a systematic study of all the possible decay chains. Instead, we focus on two specific cases which are well motivated by the renormalisation group studies of the MSSM [41]. (a) The lightest neutralino, $\tilde{\chi}_1^0$, is

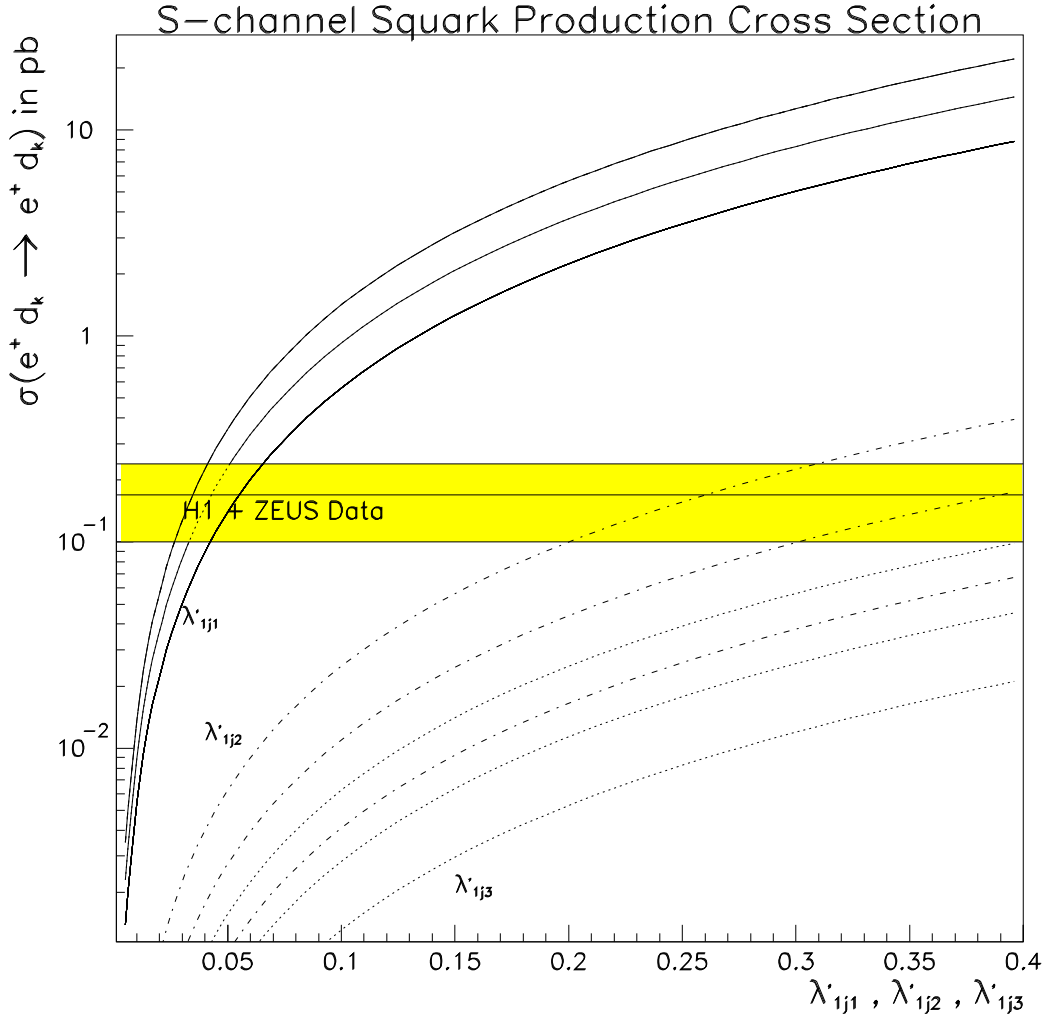


Figure 1: Excess cross-section $\sigma(e^+ d_k \rightarrow e^+ d_k)$ for a s -channel \tilde{u}_j -squark resonance for $Q^2 > 20,000 \text{ GeV}$ as a function of the coupling λ'_{1jk} for the three values of $M_{\tilde{u}_j} = 200, 210, 220 \text{ GeV}$ (top to bottom). The solid lines show the cross-sections for a non-zero coupling λ'_{1j1} (*i.e.* the d valence quark contribution), while the dashed-dotted and dotted lines show the cross-sections for the non-zero couplings λ'_{1j2} , and λ'_{1j3} (*i.e.* the s , and b sea quark contributions), respectively. Here, we assume that the only allowed squark decay mode is $\tilde{u}_j \rightarrow e^+ + d_k$. The hatched region shows the high Q^2 excess cross-section $\sigma_{ex} = (0.17 \pm 0.07) \text{ pb}$.

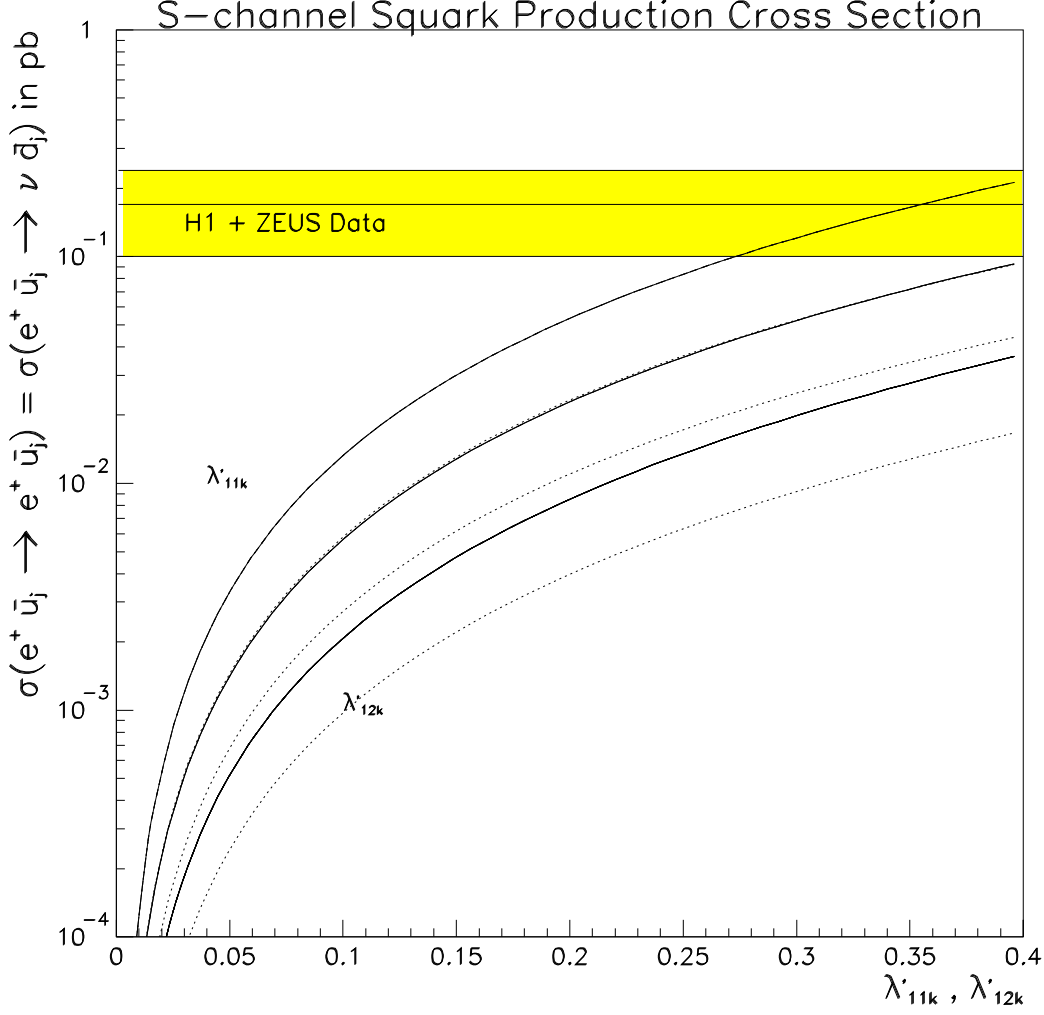


Figure 2: Excess cross-section $\sigma(e^+ \bar{u}_j \rightarrow e^+ \bar{u}_j) = \sigma(e^+ \bar{u}_j \rightarrow \nu \bar{d}_j)$ for a s-channel \tilde{d}_k -squark resonance for $Q^2 > 20,000 \text{ GeV}$ as a function of the coupling λ'_{1jk} for the three values of $M_{\tilde{d}_k} = 200, 210, 220 \text{ GeV}$ (top to bottom). The solid lines show the cross-sections for a non-zero coupling λ'_{11k} (*i.e.* the u-bar sea quark contribution), while the dotted lines show the cross-sections for the non-zero coupling λ'_{12k} (*i.e.* the c-bar sea quark contributions), respectively. Here, we assume that the only allowed squark decay modes are $\tilde{d}_k \rightarrow e^+ + \bar{u}_j$ and $\tilde{d}_k \rightarrow \bar{\nu} + \bar{d}_j$. The hatched region shows the high Q^2 excess cross-section $\sigma_{ex} = (0.17 \pm 0.07) \text{ pb}$.

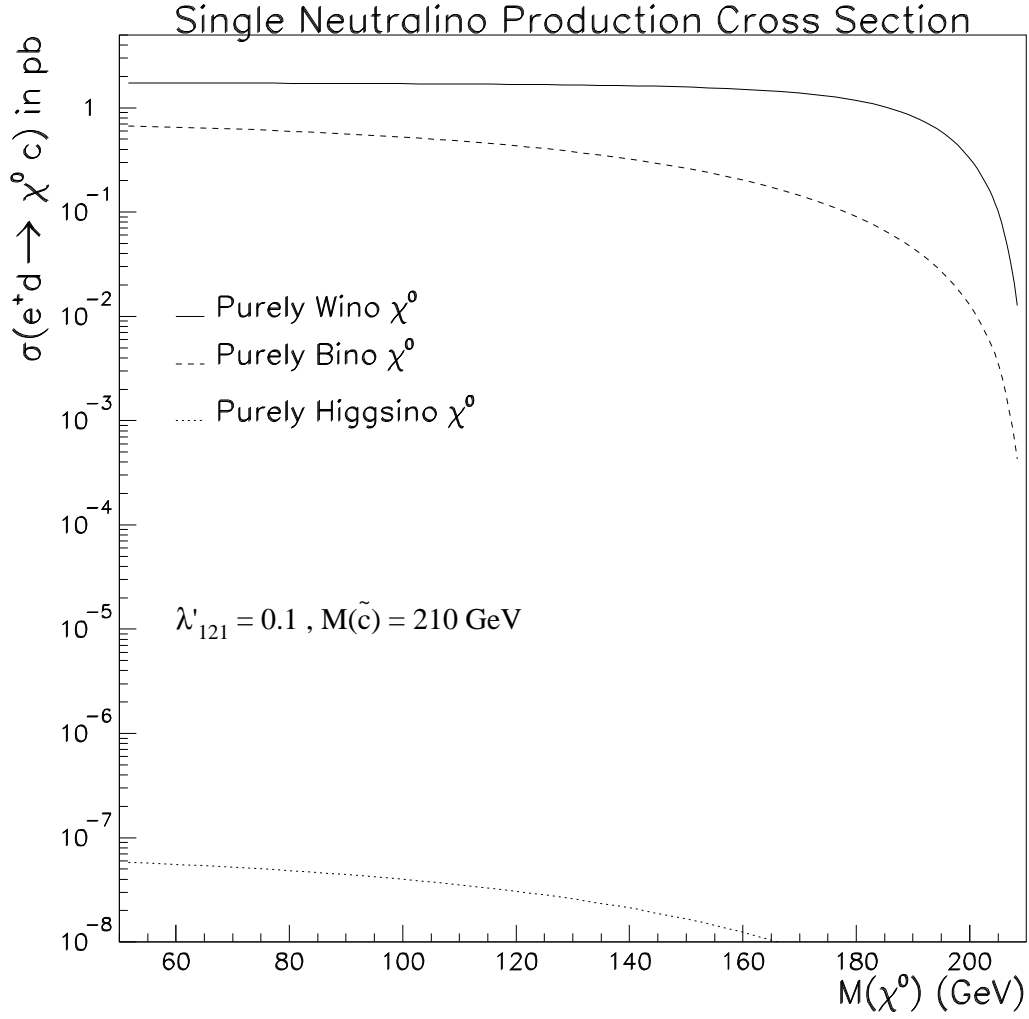


Figure 3: Cross-section $\sigma(e^+d \rightarrow \tilde{\chi}^0 c)$ for single neutralino production at HERA for the coupling $\lambda'_{121} = 0.1$ and $M_{\tilde{c}} = 210 \text{ GeV}$ as a function of the neutralino mass. The solid, dashed and dotted lines show the cross-sections for a neutralino which couples purely Wino-, Bino-, or Higgsino-like, respectively.

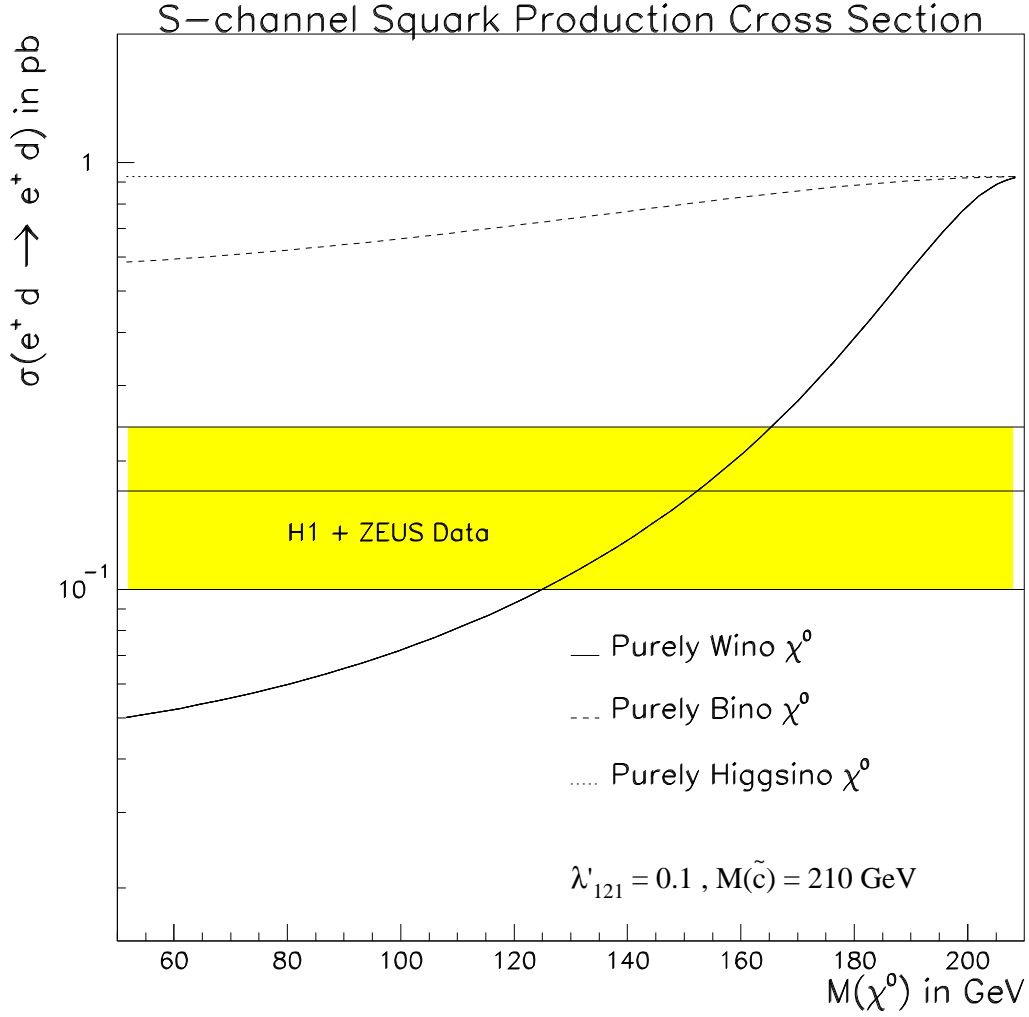


Figure 4: Effect of the additional decay mode $\tilde{c} \rightarrow \tilde{\chi}^0 c$ on the excess cross-section $\sigma_{ex}(e^+d \rightarrow e^+d)$ for a s-channel \tilde{c} -squark resonance for $Q^2 > 20,000$ GeV, $\lambda'_{121} = 0.1$ and $M_{\tilde{c}} = 210$ GeV, as a function of the neutralino mass. The hatched region shows the high Q^2 excess cross-section $\sigma_{ex} = (0.17 \pm 0.07)$ pb.

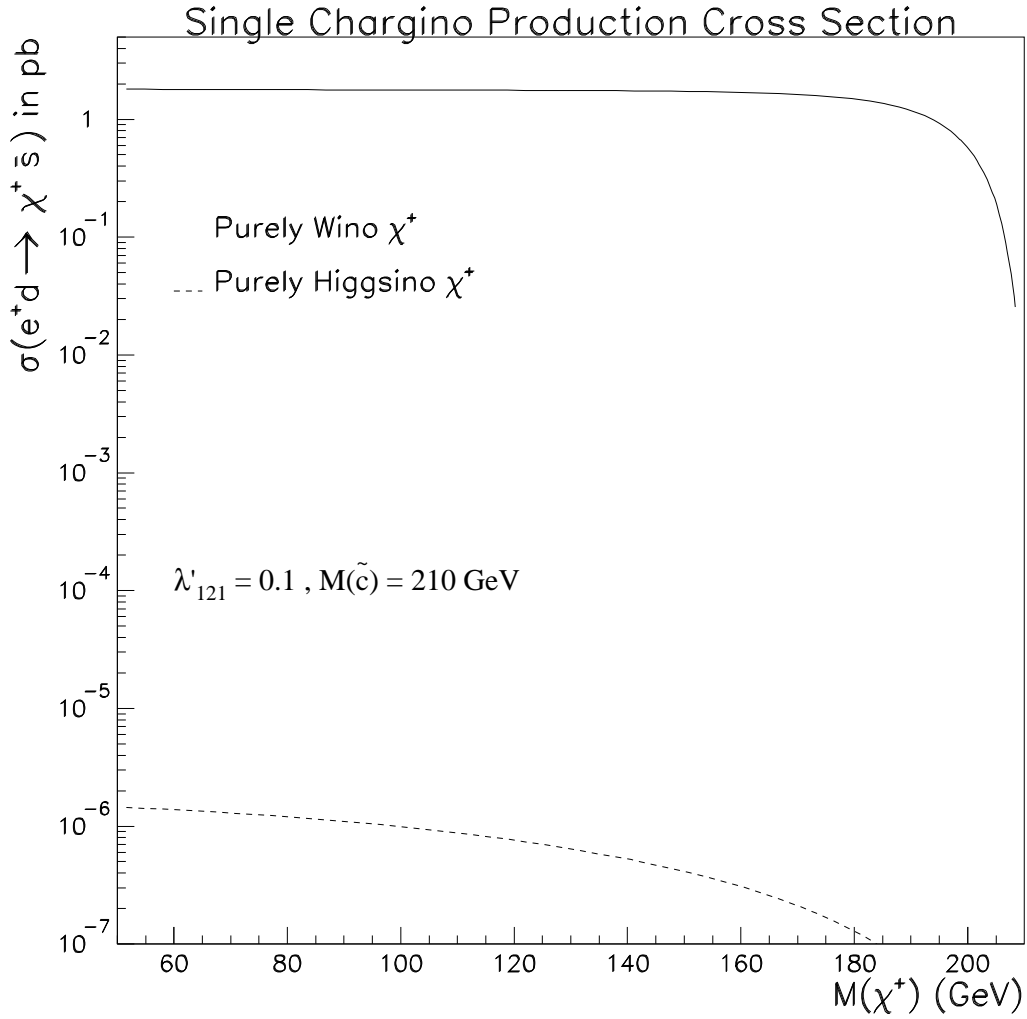


Figure 5: Cross-section $\sigma(e^+d \rightarrow \tilde{\chi}^+ s)$ for single chargino production at HERA for the coupling $\lambda'_{121} = 0.1$ and $M_{\tilde{c}} = 210 \text{ GeV}$ as a function of the chargino mass. The solid and dashed lines show the cross-sections for a chargino which couples purely Wino-, or Higgsino-like, respectively.

lighter than the produced squark, $M_{\tilde{\chi}_1^0} < M_{\tilde{u}_j}, M_{\tilde{d}_k}$ and (b) The lightest chargino, $\tilde{\chi}_1^+$, is lighter than the produced squark, $M_{\tilde{\chi}_1^+} < M_{\tilde{u}_j}, M_{\tilde{d}_k}$.

(a) If

$$M_{\tilde{\chi}_1^0} < M_{\tilde{u}_j}, M_{\tilde{d}_k}, \quad (18)$$

then we have the following additional interactions at HERA

$$e^+ + \bar{u}_j \rightarrow \tilde{d}_k \rightarrow \tilde{\chi}_1^0 + \bar{d}_k, \quad (19)$$

$$e^+ + d_k \rightarrow \tilde{u}_j \rightarrow \tilde{\chi}_1^0 + u_j. \quad (20)$$

In the second process, the case $j = 3$ is suppressed by the large top-quark mass and we do not further consider it.

The production cross section depends on the admixture of the neutralino mass eigenstate. In order to determine the cross section we focus on three special limiting cases: a purely Wino-, a purely Bino- and a purely Higgsino- $\tilde{\chi}_1^0$. In Figure 3 we plot the production cross section $\sigma(e^+ + d_k \rightarrow \tilde{\chi}_1^0 + u_j)$ as a function of the neutralino mass for these 3 special cases.⁴ We have fixed the squark mass at 210 GeV and the Yukawa coupling $\lambda'_{1j1} = 0.1$. For a purely Higgsino-neutralino, the production cross section is very small ($< 10^{-6} \text{ pb}$) and is not observable at HERA. For a gaugino-neutralino, the cross section is $\sim 1 \text{ pb}$ for neutralino masses as large as 150 GeV or 180 GeV . With the present luminosity, HERA could possibly have already produced several tens of neutralinos, upto about 30 per experiment. The neutralino decay modes are [22]

$$\tilde{\chi}_1^0 \rightarrow \{e^- u_j \bar{d}_k, e^+ \bar{u}_j d_k, \nu_e d_j \bar{d}_k, \bar{\nu}_e \bar{d}_j d_k\}. \quad (21)$$

The branching fractions are not simply 0.25 each for massless final states but sensitively depend on the admixture of the neutralino [22]. The most visible decay for a positron beam is $\tilde{\chi}_1^0 \rightarrow e^- u_j \bar{d}_k$, *i.e.* to the final state electron [11]. This requires charge identification of high p_T electrons and can be searched for in the present and upcoming data.

By including the neutralino decay of the squark we have increased the total decay width of the squark. This in turn reduces the resonant production cross sections plotted in Figure 1. In Figure 4, we show this effect for the three neutralino admixtures and for $\lambda'_{1j1} = 0.1$, $M(\tilde{u}_j) = 210 \text{ GeV}$. The change in the leptoquark-like cross section (squark LSP) is negligible for the Higgsino-neutralino. For a Bino-neutralino, the cross section can drop by about a factor two. For a Wino-neutralino the production cross section can drop by more than an order of magnitude.

If we include a Bino- or Wino- $\tilde{\chi}_1^0$ which is lighter than the produced squark, we must reconsider the solutions presented in Section 4.1. For the same coupling λ'_{1jk} , the rate for the reactions (13,15) will go down when including the neutralino. This can be compensated by increasing the Yukawa coupling, if allowed. It is only for the solutions (16.1,16.4,16.5)

⁴The single neutralino/chargino production cross-sections are quoted in the Appendix for completeness.

and (17) that this is possible. For example, for solution (16.1), producing a scalar-charm quark, we can raise $\lambda'_{121} = 0.04$ by a factor 2.5 to $\lambda'_{121} = 0.1$. We then obtain a new solution for a purely Wino- $\tilde{\chi}_1^0$ with mass $M_{\tilde{\chi}_1^0} = 125 - 165 \text{ GeV}$. This can be seen in Figure 4. The branching ratio for the direct decay $\tilde{c} \rightarrow e^+ d$ is reduced to about 0.1. For a purely Bino- $\tilde{\chi}_1^0$ only a modest increase in coupling can be allowed, otherwise the suppression is not sufficient.

We can similarly consider the effects of the decay $\tilde{d}_k \rightarrow \tilde{\chi}_1^0 + \bar{d}_k$ on the production cross section $\sigma(e^+ \bar{u}_j \rightarrow e^+ \bar{u}_j)$. The $SU(2)$ singlet d -squark only couples significantly to a purely Bino- $\tilde{\chi}_1^0$. This only leads to marginal affects, as seen above. Except for the two squark solution (17), these solutions are already marginal and we do not further consider them.

(b) We can repeat the analogous analysis for a chargino with

$$M_{\tilde{\chi}_1^+} < M_{\tilde{u}_j}, M_{\tilde{d}_k}, \quad (22)$$

in which case we obtain the additional interactions

$$e^+ + \bar{u}_j \rightarrow \tilde{d}_k \rightarrow \tilde{\chi}_1^+ + \bar{u}_k, \quad (23)$$

$$e^+ + d_k \rightarrow \tilde{u}_j \rightarrow \tilde{\chi}_1^+ + d_j. \quad (24)$$

Here we also allow for the case $j = 3$. We consider the two limiting cases, where the chargino is pure Wino- $\tilde{\chi}_1^+$ or pure Bino- $\tilde{\chi}_1^+$. In Figure 5 we plot the single chargino production cross section $\sigma(e^+ d_k \rightarrow \tilde{\chi}_1^+ \bar{d}_j)$ for these two cases for $\lambda'_{1j1} = 0.1$, and $M(\tilde{u}_j) = 210 \text{ GeV}$. For the pure Higgsino case, the cross section is again highly suppressed. These decays can be neglected. For the purely Wino case, $\sigma(e^+ d_k \rightarrow \tilde{\chi}_1^+ \bar{d}_j) \approx 1 \text{ pb}$, for $M(\tilde{\chi}_1^+) < 180 \text{ GeV}$. This suppresses the NC-like production as in the neutralino case and we obtain additional solutions. This is particularly relevant for \tilde{t} production.

The chargino decays to

$$\tilde{\chi}_1^+ \rightarrow \left\{ \nu_e u_j \bar{d}_k, \bar{\nu}_e \bar{u}_j d_k, e^- d_j \bar{d}_k, e^+ \bar{d}_j d_k \right\}. \quad (25)$$

Again, the best search mode for a positron beam is the final state electron which can be detected at HERA.

Summarising, the solutions (16.1,16.4,16.5) as well as the special solution (17) can allow for substantial decays to gauginos. The other solutions can only allow for Higgsino-like gauginos to be lighter since the decay rates are negligible. Note that the new processes via gaugino decays to positrons and neutrinos would be reconstructed at random x and Q^2 for both NC and CC.

5 Tests at HERA

There are several tests of the R-parity violating hypothesis which can be performed at HERA.

1. If HERA is switched back to e^-p collisions the processes (13) -(15) change to their charge conjugate

$$e^- + u_j \rightarrow \tilde{d}_k \rightarrow e^- + u_j, \quad (26)$$

$$e^- + u_j \rightarrow \tilde{d}_k \rightarrow \nu_e + d_j, \quad (27)$$

$$e^- + \bar{d}_k \rightarrow \tilde{u}_j \rightarrow e^- + \bar{d}_k. \quad (28)$$

For $k = 1$ or $j = 1$ the event rates would increase or decrease, respectively by [37]

$$\begin{aligned} u(x, Q^2)/\bar{u}(x, Q^2) &\gtrsim 100, \\ &\text{for } x = 0.45, \quad Q^2 = 4 \cdot 10^4 \text{ GeV}^2. \quad (29) \\ \bar{d}(x, Q^2)/d(x, Q^2) &\approx 0.03, \end{aligned}$$

Using the e^-P data from earlier runs at HERA, the first case would exclude any solution with an incoming \bar{u} -quark. But no such solution was found due to stringent low-energy bounds. For the solutions (16.1,16.4) this change should lead to a non-observation. For the other solutions with higher generation incoming quarks, there is no difference between the $q(x, Q^2)$ distribution and the $\bar{q}(x, Q^2)$ distribution and we expect no effect.

2. In the operator $L_1 Q_j \bar{D}_k$, L_1 refers to the first generation lepton $SU(2)$ doublet superfield. Therefore, the positron in (13)-(15) is *right*-handed, and the electron in (26)-(28) is *left*-handed. Thus, when the electron/positron polarisers are installed the event rate should double or vanish depending on which polarisation is chosen for the lepton beam [9]. This effect is independent of the quark generation indices.
3. Within supersymmetry with broken R-parity, the nature of the lightest supersymmetric particle (LSP) is unknown. The decay spectrum of the produced squarks depends on the supersymmetry spectrum as a whole. In the previous Section, we considered the case where a neutralino or chargino is lighter than the squark. This leads to an additional electron (positron) signal for a positron (electron) beam, which can be searched for.

The most important conclusion from this is that HERA itself can determine the nature of the observed effect. The second conclusion we draw is that it is essential for HERA to first continue running in the present mode and *not* switch to an electron beam or run at lower energy. This way both experiments can establish whether there is a genuine effect or whether it is merely a statistical fluctuation. If HERA did switch to an electron beam and the effect is due to the production of up-like squarks from down quarks the excess would be decreased and require longer running time to establish its nature. We could then end up in one year with two separate non-significant excesses and being no-more the wiser.

6 Signals at LEP 2

In this Section we discuss three tests of the R-parity violation hypothesis at LEP 2. (1) Pair production of selectrons. The pair production of squarks at LEP 2 with $m_{\tilde{q}} = 200 \text{ GeV}$ is kinematically prohibited. Selectrons on the other hand, could be kinematically accessible at LEP without having been seen at HERA. In particular, they can decay through the same R-parity violating operator $L_1 Q_j \bar{D}_k$. With the present data samples of $L \sim 25 \text{ pb}^{-1}$ per experiment at $\sqrt{s} = 130 - 172 \text{ GeV}$, selectron masses $m_{\tilde{e}} < 70 \text{ GeV}$ are accessible [42]. (2) Gauginos, if light, can be pair produced and subsequently can decay via $L_1 Q_j \bar{D}_k$ to visible leptonic final states. (3) Virtual t-channel exchange of squarks would give a contribution to the SM process $e^+ e^- \rightarrow q\bar{q}$ [43, 44]. We investigate these three effects in the following.

6.1 Selectron pair production and the ALEPH 4-jet Anomaly

If the selectrons are lighter than the gauginos, the dominant decay channel for the Yukawa coupling size of interest is:

$$\tilde{e}_{L,R} \rightarrow u_j \bar{d}_k. \quad (30)$$

Selectron pair production would then give rise to 4-jet signals at LEP 2 through the process $\tilde{e}_L \tilde{e}_R \rightarrow (u_j \bar{d}_k)(\bar{u}_j d_k)$. This scenario has been investigated in [45], where it was found that selectron masses of $m_{\tilde{e}_L} = 58 \text{ GeV}$, $m_{\tilde{e}_R} = 48 \text{ GeV}$ could explain the anomalous invariant mass peak of 4-jet final states observed by ALEPH [46], as well as the apparent difference in mass $\Delta M \sim 10 \text{ GeV}$. It must be pointed out that the ALEPH anomaly is not seen by the other three LEP experiments, and its origin is at present not understood. In this Subsection, we will assume that the ALEPH effect is due to new physics. It is then intriguing to ask whether the HERA excess when interpreted as s-channel squark production is compatible with the above interpretation of the ALEPH 4-jet signal. In order to explain the ALEPH data there are several requirements on λ'_{1jk} [45].

(a) The solution to the ALEPH 4-jet anomaly requires the associated production of an $SU(2)$ singlet selectron (\tilde{e}_R) and an $SU(2)$ doublet selectron (\tilde{e}_L) with different mass. The \tilde{e}_R can not decay directly via the operator $L_1 Q_j \bar{D}_k$, only via the mixing with the \tilde{e}_L . If this mixing is small then for small λ' the \tilde{e}_R will be long-lived. This in turn can be observed in the ALEPH detector but wasn't. Thus the coupling must be large: $\lambda'_{1jk} > 0.01$ [45].

(b) The ALEPH 4-jet data excludes final states which contain b-quarks, and favours u,d,s quark final states; charm quarks are disfavoured, but not excluded. Including the tight constraints on λ'_{111} one arrives at three solutions: λ'_{112} , λ'_{121} , λ'_{122} (*c.f.* Table 2). The solution with $\lambda'_{112} \gtrsim 0.01$ is favoured by the ALEPH data [45].

As discussed in Section 4, the HERA high Q^2 excess, too, can be explained by one of the three couplings (*c.f.* Table 3).

In order to fit the ALEPH data comfortably, the coupling λ'_{121} should be as large as possible. This evades the effects of lifetime (which are now amplified by the presence of

Coupling	Process which can explain the ALEPH 4-jet anomaly
$\lambda'_{112} \gtrsim 0.01$	$\tilde{e}_L \tilde{e}_R \rightarrow u \bar{u} s \bar{s}$
$\lambda'_{121} > 0.01$	$\tilde{e}_L \tilde{e}_R \rightarrow c \bar{c} d \bar{d}$
$\lambda'_{122} > 0.01$	$\tilde{e}_L \tilde{e}_R \rightarrow c \bar{c} s \bar{s}$

Table 2: Allowed couplings which can explain the ALEPH 4-jets.

Coupling	Process explaining the HERA high Q^2 anomaly	Additional signals at HERA
$\lambda'_{121} > 0.04$	$e^+ d \rightarrow \tilde{c} \rightarrow e^+ d$	$e^+ d \rightarrow \tilde{c} \rightarrow \tilde{\chi}^0 u$ (or $\tilde{s} \tilde{\chi}^+$)

Table 3: Allowed coupling which can explain the HERA high Q^2 anomaly.

charm in the 4-jet final states). But for a large coupling (say $\lambda'_{121} = 0.1$), the HERA excess cross-section of $0.17 pb$ only fits the predicted cross-section if the squark coupling to the neutralino is large. The additional decay mode $\tilde{c} \rightarrow \tilde{\chi}^0 c$ must reduce the predicted cross-section $\sigma(e^+ \bar{u} \rightarrow \tilde{c} \rightarrow e^+ \bar{u})$ from $0.93 pb$ to $0.17 pb$ (Figure 4). A neutralino with $M_{\tilde{\chi}^0} = 125 - 165 GeV$ which couples with a dominant bino component indeed fits the data. The additional process $e^+ \bar{u} \rightarrow \tilde{c} \rightarrow \tilde{\chi}^0 c$ has a cross-section of $1.4 pb$ (Figure 3), which would predict around 50 events between the two experiment *H1* and *ZEUS* in the 1995/1996 data; a signal which should be observable. That cross-section decreases, as the value of λ'_{121} is decreased, since the neutralino mass has to be increased correspondingly to fit the data⁵.

We conclude that the ALEPH anomaly and the HERA excess can in principle be simultaneously explained by the coupling $\lambda'_{121} > 0.04$, although this scenario is less favoured by the ALEPH data.

6.2 Other Signals at LEP 2

Let us now discuss the constraints placed on the supersymmetric spectrum by the solutions of Eq.(16). We find four scenarios which determine the gaugino spectrum:

(a) Solution (16.1) can accommodate gauginos which are substantially lighter than $M_{\tilde{q}}$ and couple electroweakly to the squarks (e.g. non-Higgsino like).

(b) Solution (16.4) requires $M_{\tilde{\chi}^0} > M_{\tilde{t}} - M_t$, and $M_{\tilde{\chi}^+} \gtrsim M_{\tilde{t}} - M_b$.

⁵It was pointed out in [51] that cancellations in the gaugino coupling of the neutralino to the left-handed charm squark can occur in large regions of Supersymmetric parameter space. In this case decays of the squark to the chargino - which do not have the same cancellations in coupling - would play the same role as the decays to the neutralino discussed above.

- (c) All other cases require either large gaugino masses ($\gtrsim 200 \text{ GeV}$), which is of no interest to LEP 2, or
- (d) they can accommodate light gauginos with a small coupling (e.g. Higgsino-like) to the squarks.

In summary, we conclude that cases (a), (b) and (d) are interesting for LEP 2 since charginos and neutralinos could be discovered up to the kinematic limit of $\sqrt{s}/2$. LEP 2 itself however has no way of testing the R-parity hypothesis of the high Q^2 HERA excess, since the non-observation of R-parity violating SUSY at LEP 2 cannot rule out that the HERA effect is indeed a sign of a s-channel squark resonance.

6.3 Virtual Effects at LEP 2 from t-channel Squark Exchange

We quote the cross-section for this effect, which has also been studied in the literature [43, 44], in the Appendix. The magnitude of the effect is small, since the main contribution to the cross-section is proportional to λ'^2 . Figure 6 shows the contribution of t-channel \tilde{c} and \tilde{s} exchange for $M_{\tilde{q}} = 200 \text{ GeV}$ at $\sqrt{s} = 190 \text{ GeV}$ including Initial State Radiation corrections. Note, that the effect due to a \tilde{c} exchange gives a positive contribution to $\sigma(e^+e^- \rightarrow d\bar{d})$, while the \tilde{s} exchange gives a negative contribution to $\sigma(e^+e^- \rightarrow u\bar{u})$.

The overall effect on the total cross-section is shown in Table 4. We have also included a column with cross-sections including an anti-ISR cut $\sqrt{s'/s} > 0.9$, where s is the center of mass energy of the incoming lepton beams, and s' is the center of mass energy of the outgoing $q\bar{q}$ pair. The cut enhances the contribution of the t-channel squark exchange to the total $q\bar{q}$ cross-section. Nevertheless, the effect is still less than 3% for a coupling $\lambda' = 0.2$. LEP 2 can therefore only probe large Yukawa couplings. For an integrated luminosity of 400 pb^{-1} (expected to be delivered to the four experiments for the 1997 run) LEP 2 would see a three sigma effect on the total $q\bar{q}$ cross-section for couplings larger or equal than $\lambda' \gtrsim 0.2(0.4)$ for $\tilde{s}(\tilde{c})$ squark exchange respectively.

Very recently, the OPAL collaboration have performed the measurement [47]. For squark masses of 200 GeV , they are sensitive to couplings $\lambda' \gtrsim 0.4$, which is already on the verge of excluding the large coupling solutions in (16).

7 Signals at the Tevatron

There are several potential tests of the above ‘supersymmetry with broken R-parity’ hypothesis (produce one squark via operator $L_1 Q_j \bar{D}_k$) at the Tevatron: (a) t-channel squark exchange interfering with Drell-Yan production, (b) single squark production, and (c) squark pair production.

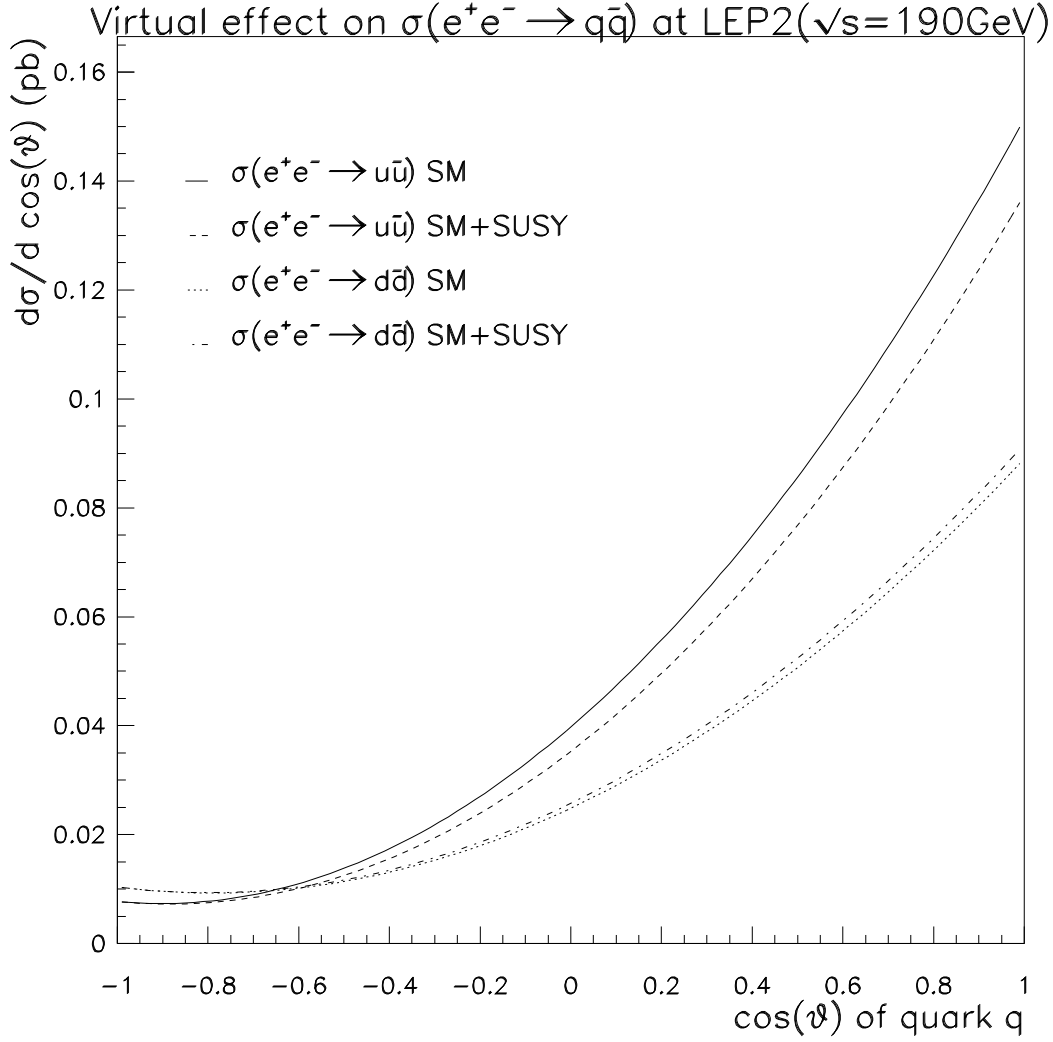


Figure 6: Differential cross-sections $d\sigma/d \cos \theta$ for $M_{\tilde{c}}, M_{\tilde{s}} = 200 \text{ GeV}$ and $\lambda' = 0.2$ respectively. We have included Initial State Radiative corrections, and used the anti-ISR cut $\sqrt{s'/s} > 0.9$ (see text).

Anti-ISR cut	$\sigma(e^+e^- \rightarrow d\bar{d})$ SM only	$\sigma(e^+e^- \rightarrow d\bar{d})$ SM plus t-channel \tilde{c} exchange	Effect on total cross-section $\sigma(e^+e^- \rightarrow q\bar{q})$
-	18.62pb	18.73pb	+0.12%
$\sqrt{s'/s} > 0.9$	3.31pb	3.42pb	+0.53%
	$\sigma(e^+e^- \rightarrow u\bar{u})$ SM only	$\sigma(e^+e^- \rightarrow u\bar{u})$ SM plus t-channel \tilde{s} exchange	
-	18.40pb	17.77pb	-0.68%
$\sqrt{s'/s} > 0.9$	5.30pb	4.77pb	-2.58%

Table 4: Cross-section values (including Initial State Radiation corrections) for the SM process and the SM plus t-channel squark exchange for $M_{\tilde{q}} = 200 \text{ GeV}$ and $\lambda = 0.2$ at $\sqrt{s} = 190 \text{ GeV}$.

(a) The operators $L_1 Q_j \bar{D}$ can also contribute to Drell-Yan production via the t -channel exchange of a squark. The dominant effect is the interference with the SM. This has been studied in [43]. However, the above study did not consider the for us relevant range at the Tevatron, basically because it was not feasible with the projected luminosity. In light of the planned Tevatron upgrade, we have repeated the analysis for our solutions. However, even for the large couplings we do not find a measurable effect ($< 5\%$) in this case.

(b) The scalar quarks can be singly produced via the parton-level processes

$$g + u_j \rightarrow e^+ + d_k, \quad (31)$$

$$g + d_k \rightarrow e^- + u_j, \quad (32)$$

as well as the complex conjugate production mechanisms. Here g denotes a parton gluon. This is completely equivalent to single leptoquark production at the Tevatron which has been analysed in [48]. The production cross section is proportional to $\lambda'_{1jk}{}^2$. For $\lambda'_{1jk} = 0.1$ and $M_{LQ} = 200 \text{ GeV}$, we have $\sigma = 0.02 \text{ pb}^{-1}$ [48] for an incoming first generation quark. Thus for our preferred solutions with $\lambda'_{121}, \lambda'_{131} = 0.04 (0.1)$ we do not expect any observable signal. For our more marginal solutions we have incoming sea-quarks which significantly suppresses the cross section. Thus even for $\lambda' = 0.3, 0.4$, we do not expect an observable cross section.

(c) Squarks can be pair produced at the Tevatron via⁶

$$g + g \rightarrow \tilde{q} + \tilde{\bar{q}}, \quad (33)$$

$$q + \bar{q} \rightarrow \tilde{q} + \tilde{\bar{q}}. \quad (34)$$

⁶The second process includes t -channel electron exchange via the R-parity violating operator. For the couplings we consider this contribution is negligible.

If the squark only decays via the dominant first lepton generation R-parity violating operator $L_1 Q_j \bar{D}_k$ then this is equivalent to first generation leptoquark production and decay. $D0$ have recently updated their analysis [49] and obtained preliminary lower bounds on such a leptoquark⁷

$$\begin{aligned}
D0 : \quad & M_{LQ} > 175 \text{ GeV}, \quad \text{for } BR(\phi_{LQ} \rightarrow e^\pm q) = 1, \\
& M_{LQ} > 147 \text{ GeV}, \quad \text{for } BR(\phi_{LQ} \rightarrow e^\pm q) = 0.5, \\
& M_{LQ} > 71 \text{ GeV}, \quad \text{for } BR(\phi_{LQ} \rightarrow e^\pm q) = 0.0.
\end{aligned} \tag{35}$$

The first bound applies for a two-body leptonic branching ratio of 1, *i.e.* the only decay mode is $\phi_{LQ} \rightarrow e^\pm + q$. This can immediately be reinterpreted as a lower bound for up-like squarks, provided they can not decay via gauginos or other supersymmetric particles. The second, weaker bound applies to the case where there is a second decay without a charged lepton and which has equal decay width to the charged lepton decay. This can be reinterpreted as a lower bound for d-like squarks, since as shown in Eqs.(13,14) they have two equal decay modes (provided the final state quark masses can be neglected).

Before applying these bounds we note that they only employ the tree-level cross-section for leptoquark pair-production. In our case, for squark pair production, the next-to-leading order calculation has been done. The production cross section is increased by ≈ 2 [50]. If we include this in the $D0$ -plot the more stringent bound increases by about 20 GeV to 195 GeV . This should be further strengthened by combining the $D0$ and CDF leptoquark bounds, and can most likely significantly cut into our required mass range (12). With the Tevatron upgrade the entire mass range can be covered.

For the down-like squarks, which have a decay branching ratio to charged leptons < 0.5 these $D0$ bounds are not relevant and our previous analysis of Section 4.1 applies. For the up-like squarks with only R-parity violating decays, solutions (16.1,16.2,16.4,16.5) and (17), these bounds apply directly and are relevant. At present they do not exclude any solution, but after combining the numbers of $D0$ and CDF the low-mass range of our solutions could be excluded. In this case one must include the gaugino decays of the squarks. As discussed in Section 4.2, the branching ratio $BR(\tilde{c} \rightarrow e^+ + d)$ can be reduced to 0.1 for $\lambda'_{121} = 0.1$ and a neutralino mass $\approx 165 \text{ GeV}$. In this case there are no relevant bounds from the Tevatron.

8 Conclusions

We have discussed the recently observed excess at HERA in the high Q^2 data in the light of supersymmetry with broken R-parity. We have two solutions which are in good agreement with all the data:

- $\lambda'_{121} > 0.04$ and the production of a scalar charm quark, \tilde{c} . If the \tilde{c} is the LSP this solution can most likely be tested at the Tevatron by combining all the existing data,

⁷These numbers are from March, 1997.

otherwise with the upgrade. If it is not the LSP, then the \tilde{c} can decay to a neutralino or a chargino. The resulting spectrum can not be tested at the Tevatron with the leptoquark pair production search. The neutralino production however should be testable at HERA with a cross section of $\mathcal{O}(1 pb)$. The signal is a charged lepton of opposite sign to the beam lepton.

- $\lambda'_{131} > 0.04$ and the production of a scalar top quark, stop, \tilde{t} . The possible solutions are analogous to the scalar charm with the exception that the decay to the neutralino is kinematically prohibited in most cases. In the renormalisation group studies in the MSSM a chargino LSP is disfavoured. Again the stop-LSP solution can be tested at the Tevatron and for a light chargino at HERA via chargino decay to an electron or positron.

We also have a set of further solutions which involve larger values of the coupling. If some of the model dependent bounds we have discussed indeed hold, these solutions are excluded. For the model independent indirect lower bounds these solutions are still viable.

- $\lambda'_{123} = 0.4$ and the production of scalar charm quarks, \tilde{c} . This solution prefers the lower mass range of the resonance solution to the HERA data ($< 210 GeV$). If the \tilde{c} is the LSP, then the dilepton search at the Tevatron can possibly test this model with the present data, if both experiments are combined. It can most certainly test it with the upgrade.
- $\lambda'_{123} = 0.4$ and the production of scalar bottom quarks, \tilde{b} . This solution also prefers the lower mass range ($< 210 GeV$). It can not be tested at the Tevatron since the charged leptonic branching ratio is less than 1/2. However this solution can be tested by the t-channel process at LEP 2.
- $\lambda'_{132} = 0.3$ producing a \tilde{t} squark. This solution allows for the full mass range. As for the \tilde{c} , this model can be tested at the Tevatron if the squark is the LSP. If it is not the LSP there is room in the coupling to allow for stop decays via the chargino (neutralino decays are kinematically forbidden or suppressed by the top quark).

We have one further solution: $\lambda'_{123} = 0.28$ and the production of two kinds of squarks, a \tilde{c} and a \tilde{b} . The tests are analogous to those discussed above for the separate solutions ($\lambda'_{123}, \tilde{c}$) and ($\lambda'_{123}, \tilde{b}$).

It is amusing to note that in Ref.[20] models with an anomaly-free family dependent $U(1)_R$ R-gauge symmetry were constructed which predicted the dominant R-parity violating operators $L_1 Q_1 \bar{D}_2$, and $L_1 Q_2 \bar{D}_1$.

We eagerly await further data to confirm or reject this hypothesis. It might then also be possible to make a statement about CC DIS and contributions from supersymmetry decays.

Acknowledgements

We thank Jon Butterworth and Ken Long for discussions of the ZEUS data. We thank Sacha Davidson for discussions on indirect bounds. We thank Gian Giudice and Michelangelo Mangano for pointing out an error in the cross section calculation in the original version.

Note Added: In our original manuscript we made a mistake in the cross section computation. The correction has led to changes in the allowed solutions. Since submitting our original manuscript several related papers have appeared [51, 52, 53]. In [51, 52] R-parity violation at HERA were also considered with similar conclusions to ours. We have also taken the opportunity to update some of the indirect bounds with more recent data and correct several typos in the formulas of the Appendix.

9 Appendix

9.1 Single Neutralino Production Cross-section at HERA

The cross-sections for the process $e^- P \rightarrow \tilde{\chi}_1^0 + X$ in the approximation where the neutralino is a pure photino have been previously calculated in [11]. In this Section, we generalise the results to the case of a neutralino (which is an admixture of the photino, wino and higgsino weak eigenstates). The differential cross-section for single neutralino production via the R-parity violating coupling λ'_{1jk} at HERA may then be written as

$$\frac{d\sigma(e^+ P \rightarrow \chi^0 + X)}{dx dQ^2} = \frac{1}{16\pi x^2 s^2} (q_d(x, Q^2) |\mathcal{M}(e^+ d_k \rightarrow \chi^0 u_j)|^2 + \bar{q}_u(x, Q^2) |\mathcal{M}(e^+ \bar{u}_j \rightarrow \chi^0 \bar{d}_k)|^2) \quad (36)$$

where $q_d(x, Q^2)$ and $\bar{q}_u(x, Q^2)$ give the probability of finding a d_k -quark and \bar{u}_j -quark respectively inside the proton; s, x, Q^2 are the center of mass energy, the Bjorken scaling variable and the momentum transfer squared. The Matrix elements can be obtained from [22] by crossing and are given by (neglecting initial state masses):

$$\begin{aligned} |\mathcal{M}(e^+ d_k \rightarrow \chi^0 u_j)|^2 &= \frac{g^2 \lambda_{1jk}^{\prime 2}}{2} \{ \\ &\frac{\hat{s}}{(\hat{s} - m_{\bar{u}_j}^2)^2 + \Gamma_{\bar{u}_j}^2 m_{\bar{u}_j}^2} [(a(u_j)^2 + b(u)^2)(\hat{s} - m_{\chi^0}^2 - m_{\bar{u}_j}^2) \\ &+ 4a(u_j)b(u)m_{u_j}m_{\chi^0}] \\ &+ \frac{m_{\bar{u}_j}^2 - u}{(u - m_{\bar{d}_k}^2)^2} [b(\bar{d})^2(m_{\chi^0}^2 - u)] \\ &+ \frac{m_{\bar{u}_j}^2 - u}{(t - m_{\bar{e}}^2)^2} [b(e)^2(m_{\chi^0}^2 - t)] \\ &- \frac{\hat{s} - m_{\bar{u}_j}^2}{[(\hat{s} - m_{\bar{u}_j}^2)^2 + \Gamma_{\bar{u}_j}^2 m_{\bar{u}_j}^2][t - m_{\bar{e}}^2]} [2a(u_j)b(e)m_{u_j}m_{\chi^0}\hat{s} \end{aligned}$$

$$\begin{aligned}
& +b(e)b(u)(\hat{s}^2 + t^2 - u^2 + (m_{\chi^0}^2 + m_{u_j}^2)(u - \hat{s} - t))] \\
& + \frac{1}{(t - m_{\tilde{e}}^2)(u - m_{\tilde{d}k}^2)} [b(e)b(\bar{d}) \\
& (t^2 + u^2 - \hat{s}^2 + (m_{\chi^0}^2 + m_{u_j}^2)(\hat{s} - t - u) + 2m_{u_j}^2 m_{\chi^0}^2)] \\
& + \frac{\hat{s} - m_{\tilde{u}j}^2}{[(\hat{s} - m_{\tilde{u}j}^2)^2 + \Gamma_{\tilde{u}j}^2 m_{\tilde{u}j}^2][u - m_{\tilde{d}k}^2]} [2a(u_j)b(\bar{d})m_{u_j}m_{\chi^0}\hat{s} \\
& + b(u)b(\bar{d})(\hat{s}^2 + u^2 - t^2 + (m_{\chi^0}^2 + m_{u_j}^2)(t - \hat{s} - u))] \} \quad (37)
\end{aligned}$$

where \hat{s}, t, u are the Mandelstamm variables defined as $\hat{s} = (p_e + p_{d_k})^2 = xs$, $t = (p_e - p_{\chi^0})^2 = -Q^2$, $u = m_{\chi^0}^2 + m_{d_k}^2 - \hat{s} - t$; $g = \frac{e}{\sin\theta_w}$; m_{χ^0}, m_{u_j} are the masses of the final state particles, and $m_{\tilde{e}}, m_{\tilde{u}j}, m_{\tilde{d}k}$ are the masses of the exchanged scalar SUSY particles; $\Gamma_{\tilde{u}j}$ is the total width of the scalar $\tilde{u}j$.

$$\begin{aligned}
|\mathcal{M}(e^+ \bar{u}_j \rightarrow \chi^0 \bar{d}_k)|^2 &= \frac{g^2 \lambda_{1jk}^2}{2} \{ \\
& \frac{m_{\tilde{d}k}^2 - u}{(u - m_{\tilde{u}j}^2)^2} b(u)^2 (m_{\chi^0}^2 - u) \\
& + \frac{\hat{s}}{(\hat{s} - m_{\tilde{d}k}^2)^2 + \Gamma_{\tilde{d}k}^2 m_{\tilde{d}k}^2} [(a(d_k)^2 + b(\bar{d})^2)(\hat{s} - m_{\chi^0}^2 - m_{d_k}^2) \\
& - 4a(d_k)b(\bar{d})m_{d_k}m_{\chi^0}] \\
& + \frac{m_{\tilde{d}}^2 - t}{(t - m_{\tilde{e}}^2)^2} b(e)^2 (m_{\chi^0}^2 - t) \\
& - \frac{1}{(t - m_{\tilde{e}}^2)(u - m_{\tilde{u}}^2)} b(e)b(u)[t^2 - s^2 + u^2 + (m_{\chi^0}^2 + m_{d_k}^2)(s - t - u) + 2m_{d_k}^2 m_{\chi^0}^2] \\
& - \frac{\hat{s} - m_{\tilde{d}k}^2}{[(\hat{s} - m_{\tilde{d}k}^2)^2 + \Gamma_{\tilde{d}k}^2 m_{\tilde{d}k}^2][u - m_{\tilde{u}j}^2]} [2a(d_k)b(u)m_{d_k}m_{\chi^0}\hat{s} \\
& - b(u)b(\bar{d})(u^2 + s^2 - t^2 + (m_{\chi^0}^2 + m_{d_k}^2)(t - s - u))] \\
& - \frac{\hat{s} - m_{\tilde{d}k}^2}{[(\hat{s} - m_{\tilde{d}k}^2)^2 + \Gamma_{\tilde{d}k}^2 m_{\tilde{d}k}^2][t - m_{\tilde{d}}^2]} [2a(d_k)b(e)m_{d_k}m_{\chi^0}\hat{s} \\
& - b(e)b(\bar{d})(s^2 + t^2 - u^2 + (m_{\chi^0}^2 + m_{d_k}^2)(u - t - s))] \} \quad (38)
\end{aligned}$$

where \hat{s}, t, u are now defined as $\hat{s} = (p_e + p_{u_j})^2 = xs$, $t = (p_e - p_{\chi^0})^2 = -Q^2$, $u = m_{\chi^0}^2 + m_{u_j}^2 - \hat{s} - t$. The total cross-section can be obtained from Eq.(36) by integrating over the x, Q^2 range

$$\begin{aligned}
x_{min} &= (m_{\chi^0}^2 + m_{f_s}^2)/s \\
x_{max} &= 1 \\
Q_{min}^2 &= \hat{s} - m_{\chi^0}^2 \\
Q_{max}^2 &= \hat{s} \quad (39)
\end{aligned}$$

and m_{f_s} is the mass of the final state quark, i.e. m_{u_j}, m_{d_k} for Eqns. (37),(38) respectively. The coupling constants a,b are given in Table A.1 of reference [22]. The cross-section for

the process $e^- P \rightarrow \chi^0 + X$ can be obtained from the above result by charge conjugation:

$$\frac{d\sigma(e^- P \rightarrow \chi^0 + X)}{dx dQ^2} = \frac{1}{16\pi x^2 s^2} (\bar{q}_d(x, Q^2) |\mathcal{M}(e^- \bar{d}_k \rightarrow \chi^0 \bar{u}_j)|^2 + q_u(x, Q^2) |\mathcal{M}(e^- u_j \rightarrow \chi^0 d_k)|^2) \quad (40)$$

where $|\mathcal{M}(e^- \bar{d}_k \rightarrow \chi^0 \bar{u}_j)|^2 = |\mathcal{M}(e^+ d_k \rightarrow \chi^0 u_j)|^2$ and $|\mathcal{M}(e^- u_j \rightarrow \chi^0 d_k)|^2 = |\mathcal{M}(e^+ \bar{u}_j \rightarrow \chi^0 \bar{d}_k)|^2$.

9.2 Single Chargino Production Cross-section at HERA

The differential cross-section for single chargino production via the R-parity violating coupling λ'_{1jk} at HERA may be written as

$$\frac{d\sigma(e^+ P \rightarrow \chi^+ + X)}{dx dQ^2} = \frac{1}{16\pi x^2 s^2} (q_d(x, Q^2) |\mathcal{M}(e^+ d_k \rightarrow \chi^+ d_j)|^2 + \bar{q}_u(x, Q^2) |\mathcal{M}(e^+ \bar{u}_j \rightarrow \chi^+ \bar{u}_k)|^2) \quad (41)$$

where the Matrix elements can be obtained from [54] by crossing and are given by

$$\begin{aligned} |\mathcal{M}(e^+ d_k \rightarrow \chi^+ d_j)|^2 &= \frac{g^2 \lambda_{1jk}^2}{4} \{ \\ &\frac{m_{d_j}^2 - t}{(t - m_{\nu}^2)^2} (\gamma_L^2 + \gamma_R^2) (m_{\chi^+}^2 - t) \\ &+ \frac{\hat{s}}{(\hat{s}^2 - m_{\bar{u}_j}^2)^2 + \Gamma_{\bar{u}_j}^2 m_{\bar{u}_j}^2} [(\delta_L^2 + \delta_R^2) (\hat{s} - m_{\chi^+}^2 - m_{d_j}^2) + 8 \mathcal{R}e\{\delta_L \delta_R^* m_{d_j} m_{\chi^+}\}] \\ &- \frac{\hat{s} - m_{\bar{u}_j}^2}{[(\hat{s} - m_{\bar{u}_j}^2)^2 + \Gamma_{\bar{u}_j}^2 m_{\bar{u}_j}^2][t - m_{\nu}^2]} \mathcal{R}e\{\gamma_L \delta_L^* [\hat{s}^2 + t^2 - u^2 \\ &+ (m_{d_j}^2 + m_{\chi^+}^2)(u - s - t)] + 2\gamma_L \delta_R^* m_{d_j} M_{\chi^+} \hat{s}\} \} \end{aligned} \quad (42)$$

where \hat{s}, t, u are defined by $\hat{s} = (p_e + p_{dk})^2 = xs$, $t = (p_e - p_{\chi^+})^2 = -Q^2$, $u = m_{\chi^+}^2 + m_{d_j}^2 - \hat{s} - t$. And

$$|\mathcal{M}(e^+ \bar{u}_j \rightarrow \chi^+ \bar{u}_k)|^2 = \frac{g^2 \lambda_{1jk}^2}{4} \frac{1}{(\hat{s}^2 - m_{d_k}^2)^2 + \Gamma_{d_k}^2 m_{d_k}^2} \epsilon_R^2 (\hat{s}^2 - \hat{s} m_{\chi^+}^2 - \hat{s} m_{u_k}^2) \quad (43)$$

where \hat{s}, t, u are defined by $\hat{s} = (p_e + p_{uj})^2 = xs$, $t = (p_e - p_{\chi^+})^2 = -Q^2$, $u = m_{\chi^+}^2 + m_{u_k}^2 - \hat{s} - t$ and the coupling constants γ, δ, ϵ are

$$\begin{aligned} \gamma_L &= iV_{12}^* \quad , \quad \epsilon_R = -\frac{im_{dk} U_{12}}{\sqrt{2} M_W \cos \beta} \\ \delta_L &= \gamma_L \quad , \quad \delta_R = -\frac{im_{d_j} U_{12}}{\sqrt{2} M_W \cos \beta}. \end{aligned} \quad (44)$$

We follow here the notation of [55], where one can find the expressions for the matrices U_{ij}, V_{ij} which diagonalise the chargino mass matrix.

9.3 Virtual Squark t-channel Exchange at LEP

The differential cross-section can be expressed as

$$\frac{d\sigma(e^+e^- \rightarrow q\bar{q})}{d\cos\theta} = \frac{d\sigma_{SM}}{d\cos\theta} + \frac{3}{32\pi s}(A_1 + A_2) \quad (45)$$

and the amplitudes are given by

$$\begin{aligned} A_1 &= \frac{\lambda^4}{4(t - \tilde{m}^2)^2} t^2 \\ A_2 &= -\frac{\lambda^2 t^2}{(t - \tilde{m}^2)} \left(\frac{e^2 Q_e Q_q}{s} + \mathcal{R}e \left\{ \frac{g_Z^2 a_e a_q}{s - M_Z^2 + i\Gamma_Z M_Z} \right\} \right) \end{aligned} \quad (46)$$

A_1, A_2 correspond to the contributions from the t-channel diagram and the SM interference respectively. Here \tilde{m} is the mass of the exchanged squark; Q_e, Q_q are the electric charge of the electron and quark q respectively; $g_Z = \frac{e}{\sin\theta_w \cos\theta_w}$; θ is the angle between the incoming electron and the quark q ; $t = -\frac{s}{2}(1 + \cos\theta)$; and a_e, a_q are coupling constants defined by

$$\begin{aligned} a_e &= -\frac{1}{2} + \sin^2\theta_w \\ a_u &= \frac{1}{2} - \frac{2}{3}\sin^2\theta_w \\ a_d &= \frac{1}{3}\sin^2\theta_w \end{aligned} \quad (47)$$

References

- [1] H1 Collaboration; ‘‘Observation of Events at very high Q^2 in ep Collisions at HERA’’; DESY 97-24; submitted to Z.Phys. C.
- [2] ZEUS Collaboration; J.Breitweg et al.; ‘‘Comparison of ZEUS Data with Standard Model Predictions for $e^+ p \rightarrow e^+ X$ Scattering at High x and Q^2 ’’; DESY 97-025; submitted to Z.Phys. C.
- [3] S. L. Adler, IASSNS-HEP-97-12, hep-ph/9702378; D. Choudhury, and S. Raychaudhuri, CERN-TH-97-026, hep-ph/9702392.
- [4] E. Eichten, K. Lane, M. E. Peskin, Phys. Rev. Lett. 50 (1983) 811.
- [5] R. Ruckl, Phys. Lett. B 129 (1983) 363; Nucl. Phys. B 234 (1984) 91.
- [6] P. Haberl and F. Schrempp, 2nd HERA Workshop, DESY, Hamburg, 1991; U. Martyn in ‘‘Future Physics at HERA’’, 3rd HERA Workshop, DESY, Hamburg, 1996.
- [7] W. Buchmuller, R. Ruckl, and D. Wyler, Phys. Lett. B 191 (1987) 442.

- [8] Separate contributions by J. Bijnens; N. Harnew; C. Berger, J. Tutas, M. Spira and P. Zerwas in the 1st HERA Workshop, DESY, Hamburg, Oct., 1987; Separate contributions by B. Schrempp; P. Schleper; B. Andrieu, V. Boudry, S. Orenstein, Y. Sirois and J. Zacek; D. Gingrich and T. Khatri in the 2nd HERA Workshop, DESY, Hamburg, Oct. 1991.
- [9] J.L. Hewett, Contributed to Proceedings of the 1990 Summer Study on High Energy Physics, Snowmass, Colorado.
- [10] J. Butterworth, and H. Dreiner, Oxford Preprint OUNP-92-01, Oct 1991, publ. in Proc. of 2nd HERA Workshop on Physics, Hamburg, Germany, Oct 29-30, 1991.
- [11] J. Butterworth and H. Dreiner Nucl. Phys. B 397 (1993) 3.
- [12] T. Kon, T. Kobayashi, Phys.Lett.B270:81-88,1991.
- [13] H. Georgi and S. L. Glashow, Phys. Rev. Lett. 32 (1974) 438.
- [14] For example: G. Senjanovic, A. Sokorac, Z. Phys. C20 (1983) 255; W. Buchmüller and D. Wyler, Phys. Lett. B 177 (1986) 377; H. Murayama, T. Yanagida (Tohoku U.). Mod. Phys. Lett. A7 (1992) 147; P. H. Frampton Mod. Phys. Lett. A7 (1992) 559; E. Baver, M. Leurer Phys. Rev. D51 (1995) 260.
- [15] E. Gildner, Phys. Rev. D 14 (1976) 1667; R. Barbieri, G.F. Giudice, Nucl. Phys. B306 (1988) 63; G. W. Anderson, and D. J. Castano, Phys.Rev. D 52 (1995) 1693.
- [16] For a review see for example H. E. Haber and G.L. Kane, Phys. Rept. 117 (1985) 75.
- [17] L.J. Hall and M. Suzuki, Nucl. Phys. B 231 (1984) 419.
- [18] S. Weinberg, Phys. Rev. D 26 (1982) 287; N. Sakai and T. Yanagida Nucl. Phys. B 197 (1982) 83; S. Dimopoulos, S. Raby and F. Wilczek, Phys. Lett. B 212 (1982) 133.
- [19] A. Yu. Smirnov, and F. Vissani, Phys. Lett. B 380 (1996) 317; J.L. Goity, and Marc Sher, Phys. Lett. B 346 (1995) 69, *ibid.* B 385 (1996) 500.
- [20] A. Chamseddine and H. Dreiner, Nucl. Phys. B 458 (1996) 65.
- [21] For example: D. E. Brahm, L. J. Hall, Phys. Rev. D 40 (1989) 2449, L. E. Ibanez, G. G. Ross, Nucl. Phys. B 368 (1992) 3; A. Yu. Smirnov, F. Vissani, Nucl. Phys. B 460 (1996) 37; A.H. Chamseddine, H. Dreiner, Nucl. Phys. B 447 (1995) 195.
- [22] H. Dreiner, and P. Morawitz, Nucl. Phys. B 428 (1994) 31.

- [23] T. Kon, K. Nakamura, T. Kobayashi, Z. Phys. C 45 (1990) 567; Acta Phys. Polon. B21 (1990) 315; T. Kon, T. Kobayashi, S. Kitamura, K. Nakamura, S. Adachi Z. Phys. C 61 (1994) 239; T. Kon, T. Kobayashi, S. Kitamura Phys. Lett. B 333 (1994) 263; T. Kobayashi, S. Kitamura, T. Kon, Int. J. Mod. Phys. A11 (1996) 1875.
- [24] E. Perez, Ph. D. Thesis, Universite de Paris, 1996.
- [25] H. Dreiner, E. Perez and Y. Sirois, Future Physics at HERA, 3rd HERA Workshop, DESY Hamburg, Sept. 1996.
- [26] M. Hirsch, H.V. Klapdor-Kleingrothaus, and S.G. Kovalenko, Phys. Rev. Lett. 75 (1995) 17; Phys. Rev. D 53 (1996) 1329.
- [27] V. Barger, G.F. Giudice, and T. Han, Phys. Rev. D 40 (1989) 2987.
- [28] S. Davidson, D. Bailey, B. A. Campbell, Z. Phys. C 61 (1994) 613.
- [29] Particle Data Group, Phys. Rev. D 54 (1996) 1.
- [30] P. Langacker, Phys Lett B256 (1991) 277.
- [31] R. M. Godbole, P. Roy, and X. Tata (Hawaii U.), Nucl. Phys. B 401 (1993) 67.
- [32] G. Bhattacharyya, J. Ellis and K. Sridhar, Mod. Phys. Lett. A 10 (1995) 1583.
- [33] K. Agashe and M. Graesser, Phys. Rev. D 54 (1996) 4445.
- [34] H1 Collaboration; Z.Phys. C71(1996)211.
- [35] We have extracted this number from the tables in [1, 2].
- [36] H. Dreiner and G.G. Ross, Nucl. Phys. B 365 (1991) 597.
- [37] A.D. Martin, R.G. Roberts, W.J. Stirling; Phys. Lett. B 354(1995) 155; RAL/95-021(95).
- [38] J. Ellis and S. Rudaz, Phys. Lett. B 128 (1983) 248.
- [39] We thank Z. Kunszt and W. J. Stirling for pointing this out to us.
- [40] D. Graudenz, M. Spira, and P.M. Zerwas Phys. Rev. Lett. 70 (1993) 1372.
- [41] This field has been extensively studied recently, as an example consider P. Ramond, R.G. Roberts, G.G. Ross, Nucl. Phys. B 406 (1993) 19, and references therein.
- [42] A.Bartl,H.Fraas,W.Majerotto, Z.Phys.C(1987) 411.

- [43] H. Dreiner, J. Ellis, D.V. Nanopoulos, N.D. Tracas, and N.D. Vlachos, *Mod. Phys. Lett.* 3A (1988) 443.
- [44] D. Choudhury, *Phys. Lett.* B376(1996)201.
- [45] M. Carena, G.F. Giudice, S. Lola, C.E.M. Wagner, preprint CERN-TH-96-352.
- [46] ALEPH Collaboration, D. Buskulic et al., *Phys. Lett.*B 388 (1996) 419.
- [47] S.Komamiya, for the OPAL collaboration, CERN seminar, Feb.25th, 1997; OPAL Collaboration, internal report PN280.
- [48] J. Hewett and S. Pakvasa, *Phys. Rev. D* 37 (1988) 3165; O.J. Eboli and A. V. Olinto, *Phys. Rev. D* 38 (1988) 3461.
- [49] D0 first generation lq-search; March 1997,
http://www-d0.fnal.gov/public/new/lq/lq_blurb.html
- [50] W. Beenakker, R. Hopker, M. Spira, and P. M. Zerwas, *Phys. Rev. Lett.* 74 (1995) 2905.
- [51] G. Altarelli, J. Ellis, G. Giudice, S. Lola, and M. Mangano, CERN-TH-97-040, *hep-ph/9703276*.
- [52] J. Kalinowski, R. Ruckl, H. Spiesberger, P.M. Zerwas, DESY-97-038, *hep-ph/9703288*.
- [53] J. Blumlein, DESY-97-032, *hep-ph/9703287*; K.S. Babu, C. Kolda, J. March-Russell, F. Wilczek, IASSNS-HEP-97-04, *hep-ph/9703299*; V. Barger, K. Cheung, K. Hagiwara, D. Zeppenfeld, MADPH-97-991, *hep-ph/9703311*; M. Drees, APCTP-97-03, *hep-ph/9703332*; J. L. Hewett, T. G. Rizzo, SLAC-PUB-7430, *hep-ph/9703337*; G.K. Leontaris, J.D. Vergados, IOA-TH-97-004, *hep-ph/9703338*; M.C. Gonzalez-Garcia, S.F. Novaes, IFT-P-024-97, *hep-ph/9703346*; D. Choudhury, S. Raychaudhuri, CERN-TH-97-51, *hep-ph/9703369*; A. E. Nelson, UW-PT-97-07, *hep-ph/9703379*.
- [54] H. Dreiner, S. Lola, P. Morawitz; *Phys. Lett.* B 389 (1996) 62.
- [55] J.F. Gunion, H.E. Haber; *Nucl. Phys.* B 272 (1986) 1.